

Effects of silica nanoparticle addition to the secondary coating of dual-coated optical fibers

J. Shiue^{a,*}, M.J. Matthewson^a, P.R. Stupak^{b,1}, V.V. Rondinella^{a,2}

^a Department of Materials Science and Engineering, Rutgers University, Piscataway, NJ 08854-8065, USA

^b SpecTran Corporation, Sturbridge, MA 01566, USA

Received 30 September 2005; received in revised form 3 February 2006; accepted 3 February 2006

Available online 30 March 2006

Abstract

The mechanical and optical properties of dual-coated optical fibers with silica nanoparticles added to the secondary (outer) coating have been investigated. Incorporation of silica nanoparticles in the secondary coating is shown to enhance the resistance of optical fibers to fatigue and zero stress aging. In contrast to the properties of single-coated fibers containing the silica additive, this beneficial effect is obtained without degrading the tensile strength. Pretreatment of the nanoparticles to improve their dispersion in the coating is also investigated. Two dispersants studied do not significantly improve dispersion and result in reduced efficiency of the mechanical reliability enhancing effect. However, improving the mechanical mixing process does produce coatings with well-dispersed nanoparticles; as a consequence a significantly reduced optical loss and a more dramatic improvement of mechanical reliability result.

© 2006 Acta Materialia Inc. Published by Elsevier Ltd. All rights reserved.

Keywords: Optical fiber; Coating; Fatigue; Stress corrosion; Aging

1. Introduction

It is well known that the strength of a fused silica optical fiber degrades when it is under an applied stress, i.e., fatigue [1,2]. This is a result of a stress-assisted chemical reaction between strained siloxane bonds and ambient moisture [3–5]. In addition, a high-strength fused silica optical fiber exhibits apparent enhanced fatigue under low stress: so-called “fatigue knee” behavior. This fatigue knee represents an abrupt transition to a substantially faster rate of fatigue at low stress that is not expected based on extrapolation from higher stress data [6–9]. The apparent fatigue parameter, n , drops from ~ 20 before the knee to ~ 7 beyond the

knee [7]. In addition to fatigue, strength degradation of high-strength fibers can occur even in the absence of any applied stress: so-called zero stress aging behavior [10]. Both the fatigue knee and zero stress aging are thought to be a result of surface roughening caused by a nanoscale non-uniform surface etching process [11–13].

Fatigue and zero stress aging are correlated with the reaction between ambient moisture and the glass surface. The widely used UV-curable acrylate coatings cannot prevent strength degradation due to their permeability to water. It has been shown by Rondinella and coworkers [14–16] that adding nanosized particles of fumed silica to the fiber coating can improve the long-term mechanical reliability of single-coated fibers. Their studies show that the coating additive can increase fiber lifetime under static fatigue, greatly delay the onset of the fatigue knee, and reduce the strength degradation due to zero stress aging. These positive effects are thought to be the result of a slowed reaction rate between the glass surface and water. Unfortunately, the particles in the coating can also degrade the tensile strength of the fiber which is likely the result of

* Corresponding author. Present address: Institute of Physics, Academia Sinica, 128 Sec. 2, Adademia Road, Nankang, Taipei 115, Taiwan. Tel.: +886 2 27896762; fax: +886 2 27834187.

E-mail address: yshiue@phys.sinica.edu.tw (J. Shiue).

¹ Now at OFS Fitel, 25 Schoolhouse Road, Somerset, NJ 08873-1207, USA.

² Now at European Commission, Joint Research Centre, Institute for Transuranium Elements, Postfach 2340, 76125 Karlsruhe, Germany.

poorly dispersed silica particles forming hard micrometer-sized agglomerates [15,16]. These agglomerates, while in contact with the glass fiber surface, generate defects that are ultimately responsible for lowering the tensile strength. In addition to the mechanical behavior, optical performance is obviously of paramount importance. The agglomerates may cause unacceptably high added microbending loss due to local application of stress to the fiber surface, while the effects on optical performance have never been systematically studied.

Optical fibers are usually coated with dual polymer layers, with the inner (primary) layer having a low elastic modulus in order to minimize microbending loss. In the work described here, we investigate the effect of adding silica nanoparticles to the outer (secondary) coating of dual-coated optical fibers. This approach is used to avoid the nanoparticles being in contact with the glass surface. The results show that keeping the nanoparticles away from the glass fiber surface can indeed preserve the high tensile strength while the long-term mechanical reliability can still be enhanced. Furthermore, we describe the effects of pretreatment of the nanoparticles and demonstrate that properly prepared nanoparticles/coating prepolymer mixtures can generate good secondary coatings which reduce added microbending loss and increase fiber lifetime. The results are explained by the better dispersion of the nanoparticles and by the consequent slower surface roughening process.

2. Experimental

2.1. Coating preparation and fiber fabrication

The commercial fumed silica nanoparticles (Cabot Corp., Tuscola, IL) used in this work have a nominal particle diameter of 5–30 nm and a specific surface area of $200 \pm 25 \text{ m}^2/\text{g}$. A prepolymer obtained from SpecTran Corp (now OFS Fitel) was used throughout as the secondary coating. The prepolymer is a liquid-phase coating material which can be cured by UV light after application onto the fiber. Table 1 summarizes the relevant properties of all coatings and the corresponding fibers reported here, including the pretreatments of the silica nanoparticles.

A pure coating containing no nanoparticles was used as the control specimen. Two groups of secondary coatings containing the nanoparticle additive were prepared for the present work.

Group (I). Three coating samples were prepared, labeled 1%, 3%, and 6%. The prepolymer was mixed with the as-received silica particles with concentrations of 1, 3, and 6 wt.%, respectively. The mixtures were then manually stirred. The control coating for comparison was labeled 0% in this group.

Group (II). Four coating specimens, labeled W, D, A, and B, containing 3 wt.% silica nanoparticles which had been subjected to different treatment procedures before addition were prepared by machine stirring. The control specimen was labeled coating C in this group. For coating W, the nanoparticles were stored in ambient environment and were considered “wet” due to the presence of absorbed moisture. For coating D, the nanoparticles were “dried” in an oven at 120 °C for two days. A weight loss of 0.64 wt.% was measured during this treatment which is attributed to the removal of surface moisture. For coating A, the particles were dried, and then treated with a commercial dispersant, 3-aminopropyltriethoxysilane (designated dispersant “a”), before it was added to the prepolymer. For coating B, the preparation procedure was similar to that adopted for coating A, except that a different dispersant, (3-glycidopropyl) trimethoxysilane (designated dispersant “b”), was used. Both dispersants a and b were obtained from Aldrich (Sigma–Aldrich Co., USA).

The procedures for the dispersant treatment were as follows. Amounts of 10 wt.% dispersant and 90 wt.% dry silica nanoparticles were separately mixed with hexane. The mixtures were then mixed together and stored in ambient environment for a week, then heated in a 50 °C oven overnight to ensure complete removal of the solvent. The dispersant/nanoparticles were then ground using a mortar and pestle. After these treatments, the particles were mixed into the liquid prepolymer by machine stirring for 3 h. All four mixtures (A, B, D, and W) were separately stored in beakers in ambient environment for a week until the air bubbles formed during the mixing process fully disappeared. The disappearance of the bubbles was determined

Table 1
Summary of the preparation procedures of the coating specimens and the corresponding fibers

Group	Coating	Silica (wt.%)	Mixing nanoparticles + prepolymer	Pretreatment of nanoparticles	Fiber label
Group I	0%	0		–	0% (reference)
	1%	1	Manual	No treatment	1%
	3%	3	Manual	No treatment	3%
	6%	6	Manual	No treatment	6%
Group II	C	0		–	Fiber C (reference)
	W	3	Mechanical	No treatment	Fiber W
	D	3	Mechanical	Dried in oven	Fiber D
	A	3	Mechanical	Dried + dispersant a	Fiber A
	B	3	Mechanical	Dried + dispersant b	– ^a

^a This coating did not fully polymerize during fiber drawing, and was finally discarded.

by visual inspection. During the whole process, the prepolymer was covered with an opaque material to prevent UV light causing premature curing.

All the coating specimens were used as secondary coatings for 125 μm diameter multimode (MM) silica optical fibers. Fibers from groups (I) and (II) were drawn on an R&D draw tower at two different times. However, all fibers were drawn with the same draw speed, draw tension, primary coating, and coating cure condition. The primary and secondary coating diameters were 200 and 250 μm, respectively.

2.2. Mechanical and optical characterization techniques

Three aspects of the mechanical properties of the fibers were investigated: zero stress aging, static fatigue, and tensile strength. The fatigue and aging experiments were carried out at 90 °C in pH 7 buffer solution. Such a high-temperature environment was selected as it accelerates the kinetics of the reaction between water and the fiber surface. Buffer solution was used to avoid the complication of additional pH effects, since it has been shown that the pH affects fatigue and aging results [2]. Several specimens were tested under each condition and the average values are reported. The 95% confidence intervals were found to be small, of the order of the size of the plotted point in the figures, and thus have been omitted for clarity.

For the aging experiments, the fibers were immersed in 90 °C pH 7 buffer solution under zero applied stress for times varying from 0 to 100 days. The residual strength after aging was then measured in 25 °C pH 7 buffer using a dynamic two-point bend technique at a faceplate speed of 1000 μm/s [17–19]. Fifteen specimens were tested for each condition. The static fatigue experiments were performed in 90 °C pH 7 buffer solution at various applied stresses, using a two-point bend technique [20,21]. Twenty specimens were tested for each condition. Tensile strength was measured for a gage length of 0.5 m in a temperature- and humidity-controlled box at 25 ± 0.5 °C and 50 ± 5% relative humidity at a constant strain rate of 4%/min. Thirty specimens were tested for each fiber to obtain strength distributions.

The optical loss in the fibers was measured using the “basketweave” technique [22] which approximates the added microbending loss expected after making an optical fiber cable. The technique involves winding a number of kilometers of fiber under tension onto a spool using a coarse lay such that the fiber is subjected to many small-amplitude bends at the fiber/fiber crossovers. The added optical loss was determined from the difference between the fiber loss measured for fiber spooled under tension on the basketweave spool and when spooled at zero tension on a 1 m circumference spool. The measurements were made at 850 nm using an optical time domain reflectometer (OTDR) and in an ambient environment for residence times on the basketweave spool varying from 0 to 26 h.

3. Results and discussion

3.1. Coating behavior during preparation

The pure liquid prepolymer with no additive (control coating) had a clear appearance. All the other coating specimens showed a whitish color, except for coating B which was slightly yellow. The viscosities of all the prepolymers with nanoparticle addition were higher than that of the pure prepolymer. A simple test was done for all the coating specimens: a laser pointer was shined through the coating samples. The light scattering was found to be significant in the 6 wt.% sample, while less obvious in the rest of the coating specimens. The scattering was further reduced in coatings A and B, indicating the dispersants did have a positive effect on dispersing the silica particles. It was found the fiber with coating B could not be fully cured under normal drawing conditions which implies that different dispersants have dif-

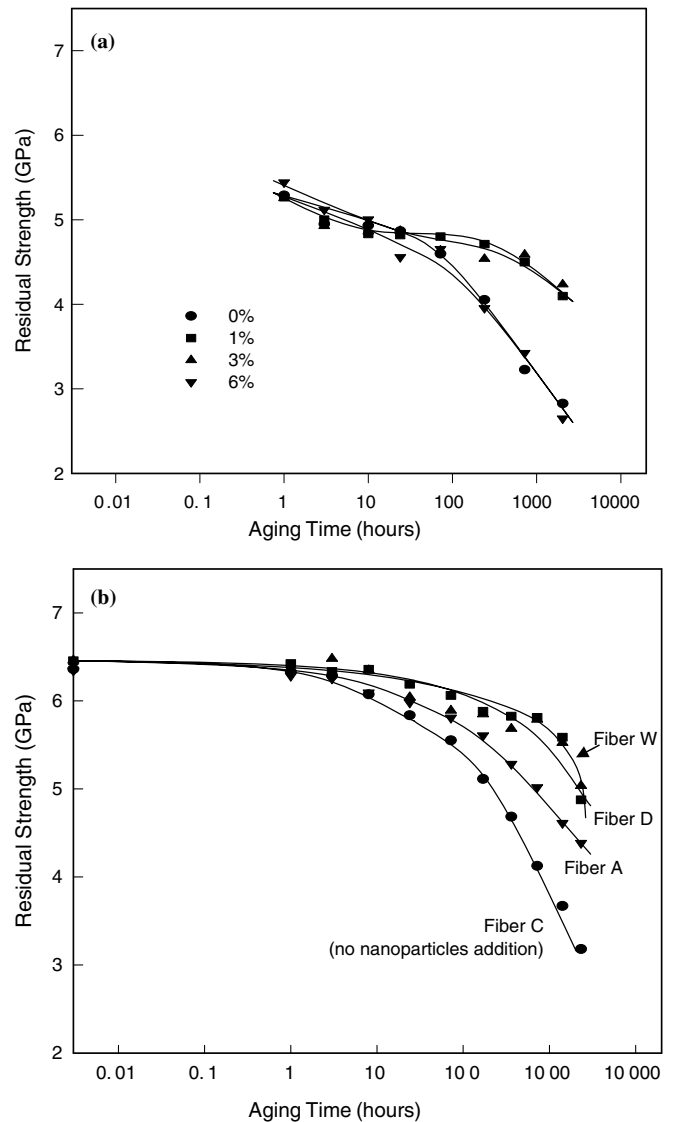


Fig. 1. Residual strength of the fibers: (a) from group (I); (b) from group (II) after zero stress aging in 90 °C pH 7 buffer solution.

ferent effects on the polymer cure. Therefore, this fiber was discarded without further tests being performed.

3.2. Mechanical behavior

3.2.1. Zero stress aging

As shown in Fig. 1(a), the zero stress aging results obtained for the group (I) fibers showed similar behavior for the specimens with 1 and 3 wt.% coating additive, both having a residual strength of ~ 4.2 GPa after 85 days. However, the fiber with 6 wt.% nanoparticles in the coating showed behavior similar to that of the 0 wt.% sample. The residual strength of 0 and 6 wt.% samples after 85 days aging was ~ 3 GPa. Such a high concentration of nanoparticles does not have positive effects on the fiber. The most likely possibility is that the concentration of the agglomerates formed in the 6 wt.% coating mixture is relatively high, which is verified by the obvious light scattering phenomenon as described above. The formation of the agglomerates perhaps resulted in some silica-free regions after the coating mixture was applied onto the fiber, and thus reducing the protective effect. Further studies of the mechanical behaviors were thus performed only on the fibers from group (II) to understand the effects of the treatment.

Fig. 1(b) shows the residual strength of the fibers with pre-treated nanoparticles in the secondary coating after zero stress aging. The strength of the control fiber, C, degraded significantly faster than that of the other fibers. After 100 days of aging, the residual strength was ~ 5 GPa for fibers W and D, ~ 4.4 GPa for fiber A, and ~ 3 GPa for fiber C. Strengths below around 3 GPa are of practical concern, since it can be difficult to handle such a weak optical fiber in the field without breaking it. These results are compared and discussed with the static fatigue results in the next section.

3.2.2. Static fatigue

The time to failure in the static fatigue experiments is shown in Fig. 2 as a function of applied stress. All the fibers with nanoparticle additions survived longer than fiber C, the control fiber. The onset of the fatigue knee is delayed for all the fibers with nanoparticle addition, by an order of magnitude or more in time. Fiber A shows better long-term mechanical performance than fiber C, but the effect is not as large as for fibers W and D. Fibers W and D have similar times to failure under high applied stress (>2.5 GPa), while at lower applied stress the two fibers show somewhat different behavior: a more abrupt knee is observed for W, while for D a much gentler change of slope is observed. These results show the same trends as shown by the aging behavior in Fig. 1(b).

The difference between the aging and fatigue behavior of fibers W and D suggests that, at least before the onset of the knee at $\sim 10^7$ s, the amount of moisture absorbed by the particles before incorporation in the coating does not have a large effect. While there might be some difference in the behavior beyond the knee, this is not conclusive because of the limited data obtained at such long experimental durations.

Previous studies using atomic force microscopy surface analysis [14] showed that the surface of an aged fiber with silica addition in the coating has an rms roughness of 0.46 nm, which is significantly smoother than the surface roughness (1.36 nm rms) of the aged fiber without silica addition in the coating [14]. The surface roughness corresponds to the fiber strength [12], indicating the silica particles in the coating can prolong the fiber strength by slowing the fiber surface roughening process, i.e., the dissolution of the glass fiber surface. The dissolution rate of silica in water has been extensively studied [23,24]. While the factors involved in the dissolution process are rather complicated, the dissolution rate in general increases with increasing specific surface area of silica and pH values [23]. It is therefore, reasonable to assume water would preferably react with the silica nanoparticles than the fiber surface. However, it is unlikely such low concentrations of the silica additives can impede water from reaching the fiber surface in such a long experimental time, since the acrylate coating is known to be highly permeable to water. Therefore, a more reasonable guess is that the reaction products of the silica nanoparticles and water would change the local pH environment on the fiber surface, hence reduce the dissolution rate of the surface. A recent study of the diffusion of moisture through polymer coatings showed that the nanoparticles in the secondary coating do not affect moisture permeability [25], also suggesting that the nanoparticles do not slow surface roughening by reducing the rate of water diffusion to the fiber surface.

The intermediate results for fiber A, as shown in Figs. 1(b) and 2, indicate that dispersant may promote stronger adhesion between the particles and the polymer, thereby making the particles less reactive with water.

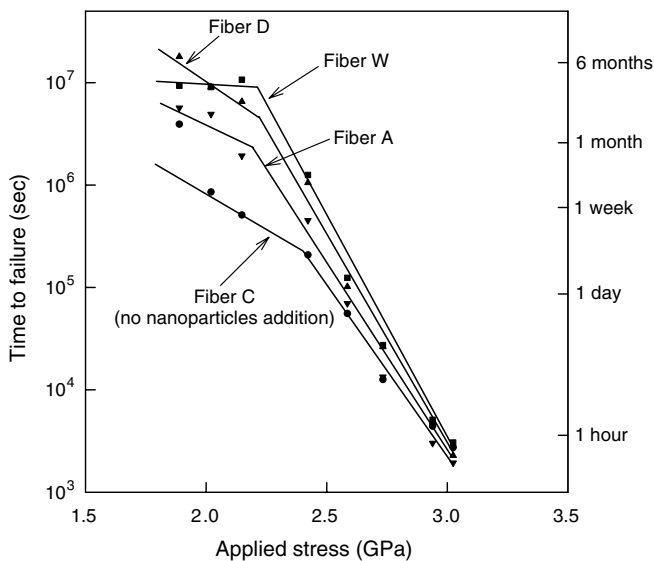


Fig. 2. Static fatigue in two-point bending of the fibers measured in 90 °C pH 7 buffer solution.

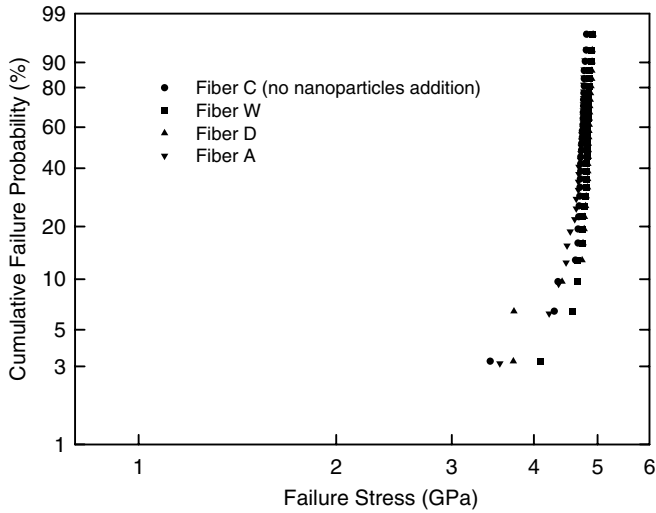


Fig. 3. Tensile strength of dual-coated fibers with silica nanoparticles in the secondary coating.

The most significant aspect of the results presented here is that the silica nanoparticles in the secondary coating, even if they are not in close proximity to fiber surface, can still have positive effects on long-term reliability.

3.2.3. Tensile strength

Fig. 3 shows the Weibull distributions for the tensile strength of fibers C, W, D, and A. Each fiber had some relatively weaker specimens among the 30 specimens tested. The weak flaws are separated on a length scale of meters and were not observed in two-point bend testing because of the very short test length. This phenomenon is not related to the addition of the nanoparticles, since the fiber with no additive (fiber C) also shows the same behavior. These occasional defects are therefore not relevant to the current study. For comparison, data for the tensile strength of two single-coated fibers from earlier work [16] are shown in Fig. 4, in which one fiber has no nanoparticles and the

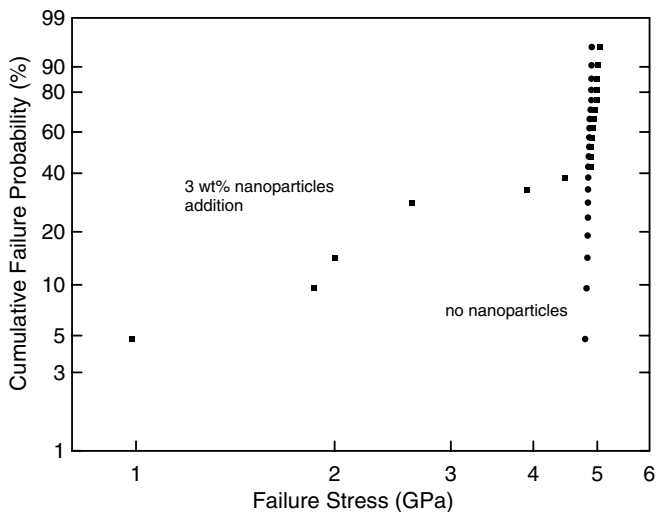


Fig. 4. Tensile strength of single-coated fibers with and without silica nanoparticles in the coating.

other one has 3 wt.% nanoparticles. The results shown in Fig. 4 were obtained using 0.3 m gage length and a strain rate of ~10%/min in ambient environment. The small difference in test length (0.3 vs. 0.5 m) does not explain the difference between Figs. 3 and 4. The broad low strength mode of the single-coated fiber with coating additive, as shown in Fig. 4, is likely to be a result of particles in contact with the fiber surface. In contrast, the dual-coated fibers (Fig. 3) do not have such low tensile strength mode.

3.3. Microbending loss

In this work, 62.5/125 μm graded index MM fiber was used to characterize the added microbending loss due to the presence of the nanoparticles in the coating. MM fiber was chosen since it generally exhibits a smoother and more repeatable optical power loss vs. distance response (measured using the OTDR) than single-mode fiber.

Fig. 5 shows the added optical loss of the group (I) fibers. The added microbending loss decreases with the fiber residence time on the basketweave spool for all specimens. This behavior can be explained by the relaxation of the winding tension by viscoelastic deformation of the polymer coating [22]. It is clear that the added loss increases with increasing nanoparticle concentration. The added loss at 850 nm ranges from ~0.5 dB/km for 1 wt.% additive to ~6 dB/km for 6 wt.% additive. These unacceptably high optical losses are probably caused by poor dispersion as a result of large silica agglomerates.

Fig. 6 shows the added microbending loss of the group (II) fibers. The dashed line shows the 3 wt.% result from Fig. 5 for comparison. The control fiber C, with no nanoparticles added, exhibits a small added loss of less than 0.1 dB/km. Fibers W, D, and A all show significantly lower losses than the results in Fig. 5, indicating that a simple process change from hand-stirring to machine-stirring can

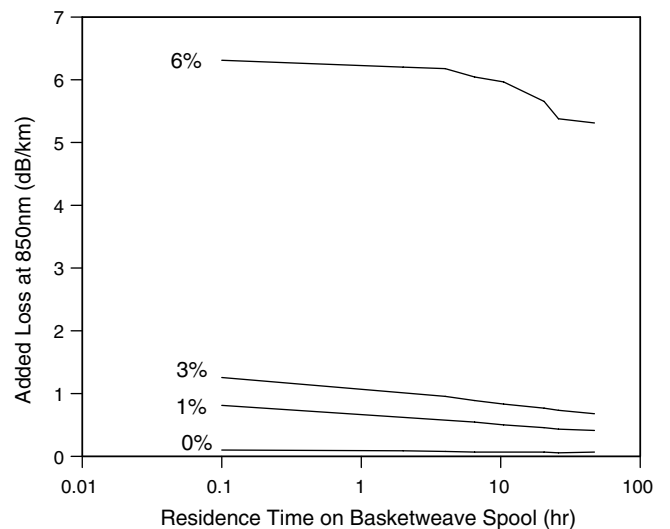


Fig. 5. Added optical loss of the fibers with various concentrations of non-pretreated nanoparticles added to the secondary coating. Particles were incorporated using hand mixing.

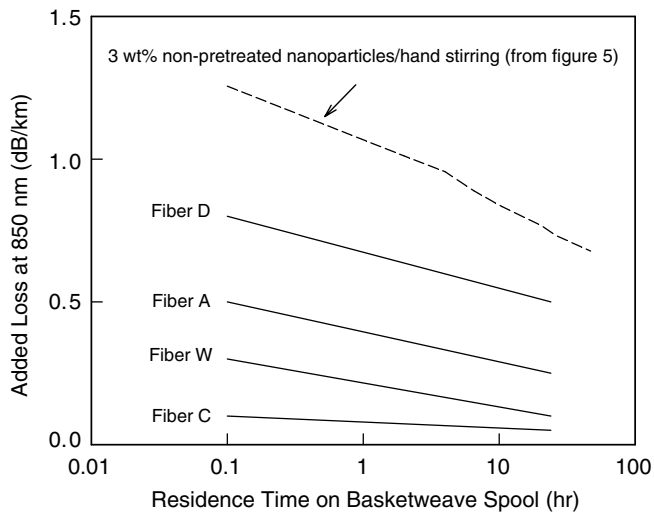


Fig. 6. Added optical loss of the fibers with secondary coatings containing 3 wt.% of nanoparticles with various pretreatments. Particles were incorporated using machine mixing.

produce significant improvement of the final properties by achieving better dispersion and reducing the added loss.

The pretreatment effects can also be observed in Fig. 6. Fiber W has the lowest loss, fiber D has the highest loss, and fiber A shows intermediate behavior. These results suggest that the as-received silica nanoparticles have fewer and smaller agglomerates. The drying process used on the nanoparticles for fibers A and D causes the formation of some agglomerates which result in higher added loss, though the dispersant does partially counteract this. The effects of the nanoparticle pretreatment considered here on the optical performance point to the conclusion that relatively simple improvements in the coating preparation (e.g., mechanical mixing techniques) might work better for dispersing the as-received nanoparticles. The chemical procedures, although helping dispersion a little, also reduce the improvement in the mechanical reliability caused by the nanoparticles.

4. Conclusions

Silica nanoparticles were added into the outer coating of dual-coated fibers and the effects on optical and mechanical properties of the fibers have been investigated. Earlier work showed that the addition of silica nanoparticles to the polymer coatings on single-coated optical fibers significantly reduces the strength degradation that occurs upon long-term aging of the fibers in aggressive environments. The suggested mechanism for this effect is that the particles reduce the rate of roughening of the fiber surface by preferentially reacting with water due to their high specific surface area, the reaction products then reduce the dissolution rate at the fiber surface by changing the local pH environment. However, it was found that the particles resulted in unacceptable degradation of the tensile strength [15]. The

results presented here show that these negative effects can be overcome. The tensile strength is shown to be improved by incorporating the particles in the outer, secondary polymer coating where they are not in mechanical contact with the glass surface. Even though the particles are now removed from the glass surface, they are shown to still provide considerable protection from strength degradation in aggressive environments. It is found that various pretreatments of the particles, including the use of dispersants, can affect the properties of the resulting fiber. The increased microbending loss caused by the particle addition can be considerably reduced by improving the mixing techniques. Such optical loss is low enough to be acceptable for a range of specialty optical fiber applications and could prove useful in applications where the fiber is exposed to harsh environments.

Acknowledgements

The authors thank Dr. Remco van Weeren for suggestions concerning the wetting agents and Michael J. O'Connor, Donna J. Morgan, B. Bellerive, and Juan Ruiz for assistance with making the measurements.

References

- [1] Kurkjian CR, Krause JT, Matthewson MJ. *J Lightwave Tech* 1989;7:1360.
- [2] Matthewson MJ, Kurkjian CR. *J Am Ceram Soc* 1988;71:177.
- [3] Charles RJ. *J Appl Phys* 1958;29:1549.
- [4] Michalske TA, Freiman SW. *J Am Ceram Soc* 1983;66:284.
- [5] Duncan WJ, France PW, Craig SP. In: Kurkjian CR, editor. *Strength of inorganic glass*. New York, (NY): Plenum Press; 1985. p. 309.
- [6] Wang TT, Zupko HM. *J Mater Sci* 1978;13:2241.
- [7] Krause JT. *Proc 5th Eur Conf Opt Commun* 1979;19.1-1.
- [8] Chandan HC, Kalish D. *J Am Ceram Soc* 1982;65:171.
- [9] Krause JT, Shute CJ. *Adv Ceram Mater* 1988;3:118.
- [10] Krause JT. *J Non-Cryst Solids* 1980;38–39:497.
- [11] Kurkjian CR, Krause JT, Paek UC. *J de Phys* 1982;43:C9-585.
- [12] Robinson RS, Yuce HH. *J Am Ceram Soc* 1991;74:814.
- [13] Yuce HH, Varachi JP, Jr., Kilmer JP, Kurkjian CR, Matthewson MJ. *OFC'92 Tech Digest* 1992; postdeadline paper.
- [14] Rondinella VV, Matthewson MJ, Kurkjian CR. *J Am Ceram Soc* 1994;77:73.
- [15] Rondinella VV, Matthewson MJ, Foy PR, Schmid SR, Krongauz V. *Proc Soc Photo-Optv Instrum Eng* 1993;2074:46.
- [16] Matthewson MJ, Yuce HH, Rondinella VV, Foy PR, Hamblin JR. *OFC'93 Tech Digest* 1993;4:PD2187.
- [17] France PW, Paradine MJ, Reeve MH, News GR. *J Mater Sci* 1980;15:825.
- [18] Matthewson MJ, Kurkjian CR, Gulati ST. *J Am Ceram Soc* 1986;69:815.
- [19] Rondinella VV, Matthewson MJ. *J Am Ceram Soc* 1993;76:139.
- [20] Cowap SF, Brown SD. *J Am Ceram Soc* 1987;70:C-67.
- [21] Matthewson MJ, Kurkjian CR. *J Am Ceram Soc* 1987;70:662.
- [22] Stupak PR, Bellerive B. *Proc SPIE* 1995;2611:162.
- [23] Iler RK. *The chemistry of silica: solubility, polymerization, colloid and surface properties, and biochemistry*. Wiley-Interscience: New York (NY); 1979.
- [24] Vogelsberger W. *J Phys Chem B* 2003;107:9669.
- [25] Mrotek JL, Matthewson MJ, Kurkjian CR. *J Lightwave Tech* 2003;21:1775.